Journal of Nuclear Materials 377 (2008) 219–224

Contents lists available at ScienceDirect

Journal of Nuclear Materials

journal homepage: www.elsevier.com/locate/jnucmat

Liquid Pb–Bi embrittlement effects on the T91 steel after different heat treatments

B. Long [a], Z. Tong [a,b], F. Gröschel [a], Y. Dai [a,*]

[a] Paul Scherrer Institut, 5232 Villigen PSI, Switzerland
[b] China Institute of Atomic Energy, Beijing 102413, China

A B S T R A C T

The present work aims to investigate the susceptibility of ferritic/martensitic steels of different strength to the embrittlement of liquid Pb–Bi eutectic (LBE). Slow strain rate tensile (SSRT) tests on specimens of the T91 steel in three tempering conditions at 500, 600 and 760 °C were conducted in Ar and in LBE at temperatures between 150 and 500 °C. For the specimens tempered at 760 °C (the normal tempering condition) the susceptibility of the steel to LBE embrittlement appeared at temperatures between 300 and 450 °C. With increasing the strength of specimens by lowering the tempering temperature, specimens tempered at 600 and 500 °C demonstrated more pronounced embrittlement effects, reflected by wider and deeper 'ductility-troughs'. The results suggest that ferritic/martensitic steels with higher strength are more susceptible to LBE embrittlement. The LBE embrittlement effects can be attributed to the decrease of fracture stress resulted from the 'weakening inter-atomic bond' by LBE contacting at crack tips.

1. Introduction

Liquid metal embrittlement (LME) refers to the instantaneous reduction or loss of ductility of ductile materials stressed in contact with liquid metals. LME is difficult to be predicted and the mechanisms are not yet so clear despite many years of research [1]. The reason is that the embrittlement phenomena are complicated. Many parameters such as strain rate, temperature, yield stress, stress concentration, surface condition, etc. may be taken into consideration to assess the risk of the LME.

Liquid lead–bismuth eutectic (LBE) is known for its embrittlement effects on martensitic steels [2–7]. It is one of many important issues in materials research programs for developing accelerator driven system (ADS) for nuclear waste transmutation (e.g. EU 6th Frame Program – EUROTRANS), where martensitic steels (e.g. the T91 steel) are selected for structural components in contact with LBE. In the MEGAPIE (the Mega-watt pilot experiment) target R&D program, this issue was greatly emphasized, because some preliminary results illustrated more severe LBE embrittlement effects on irradiation hardened specimens [8,9]. However, due to the difficulties of handling radioactive specimens, studies on the LME of irradiated materials are still very limited. In order to improve the understanding of irradiation hardening effects or, more general, the strength effects on the LME of ferritic/martensitic steels, we have investigated LBE embrittlement effects on T91 specimens of different strengths achieved by tempering at lower temperatures. In the present paper, the results of slow strain rate tensile (SSRT) tests are described.

2. Experimental

2.1. Material and specimens

The material studied in this work is the T91 martensitic steel produced by the Ugine company, France. The chemical composition is given in Table 1. The normal heat treatment of the steel is normalizing at 1050 °C for 1 h and followed by air cooling, and tempering at 760 °C for 2 h and followed by air cooling.

Small tensile specimens with a gauge section of 0.75 × 1.5 × 5 mm were cut with an electro-discharge machine (EDM) from a 15 mm-thick plate and then finished with mechanical polishing using #1000 sandpaper. However, the edges of the specimens remained as EDM cut without additional polishing or machining. Afterwards, in order to obtain the desired strength, the specimens were re-treated in two steps: (1) normalized at 1040 °C in high vacuum for 60 min and followed by air cooling and (2) tempered separately at 760, 600 and 500 °C in high vacuum for 2 h and followed by air cooling. The three groups of specimens were named according the tempering temperatures as HT760, HT600 and HT500, respectively.

2.2. Slow strain rate tensile (SSRT) tests

The SSRT tests were performed on a Zwick mechanical testing machine with a 20 kN load capacity. A special device was developed for tensile testing in an LBE environment. The detail information about this facility was described in the previous report [7]. The tests were carried out at a nominal strain rate of 1×10^{-5}/s in both Ar and LBE environments at temperatures between 150 and 500 °C. The composition of the LBE was 44.8 wt% Pb and 55.2 wt%

* Corresponding author. Tel.: +41 56 310 4171; fax: +41 56 310 4529.
E-mail address: yong.dai@psi.ch (Y. Dai).

0022-3115/$ - see front matter © 2008 Elsevier B.V. All rights reserved.
doi:10.1016/j.jnucmat.2008.02.050

Table 1
The chemical composition of the T91 steel (Fe balance)

Element	Cr	Ni	Mo	Mn	Ti	V	Nb	Cu	C	Si	P	S	N
Content (wt%)	8.63	0.23	0.95	0.43	0.003	0.21	0.09	0.046	0.1	0.31	0.02	0.006	0.03

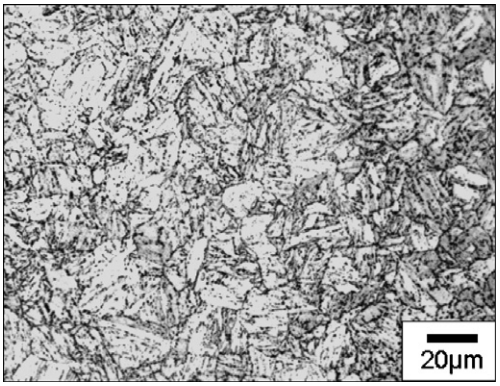

Fig. 1. Optical micrograph of the T91 steel in the normal tempering condition (tempered at 760 °C).

Bi. The impurities in the material were less than 50 wppm in total. It should be noted that the oxygen content was below 1 wppm, because the LBE was kept in the storage tank at 250 °C.

After tensile tests, the fracture surfaces of broken samples were examined using a scanning electron microscope (SEM). Prior to the SEM examination, some broken samples were cleaned in a solution which was a mixture of CH_3COOH, H_2O_2 and C_2H_5OH at a ratio of 1:1:1 to remove the LBE adhered on the fracture surfaces.

3. Results

3.1. Material characterization

The martensitic structure of the HT760 material was observed with an optical microscope. As shown in Fig. 1, it consists of martensite laths that colonized the prior austenite grain (PAG) during

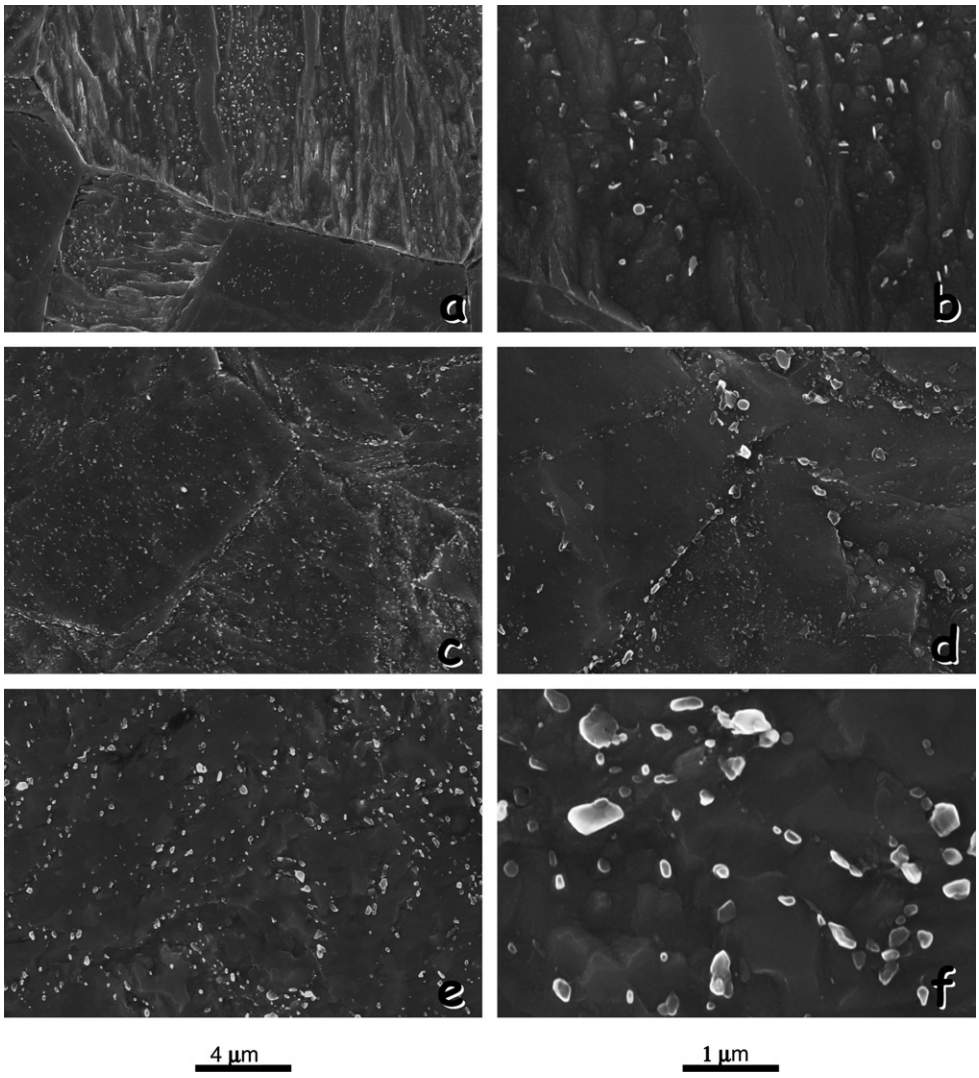

Fig. 2. SEM observation on the distribution of carbide precipitation in: (a) the HT500, (c) the HT600 and (e) the HT760 specimens. Graphs (b), (d) and (f) are of a higher magnification for (a), (c) and (e), respectively. The scales at the bottom are for the graphs in the left and right columns.

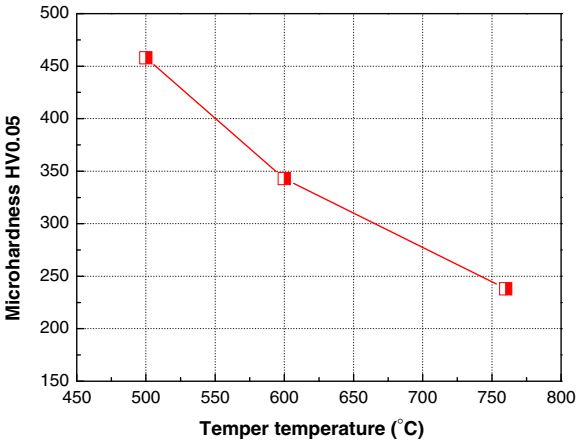

Fig. 3. Micro-hardness changes versus tempering temperature.

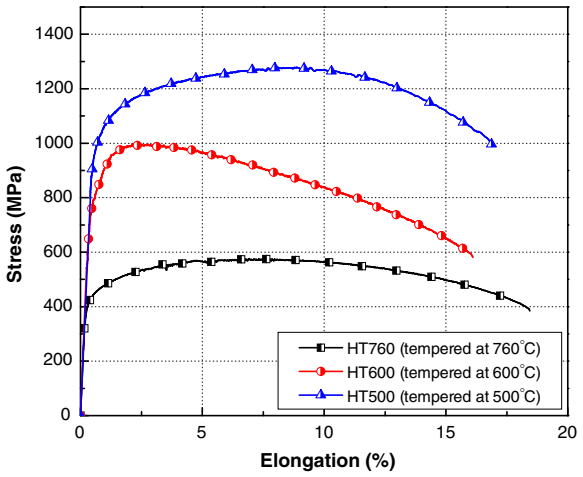

Fig. 4. Tensile stress–strain curves of T91 specimens tested in Ar at 300 °C after different tempering.

the air cooling from the normalizing temperature 1040 °C. The average PAG size is approximately 25 μm. For the HT600 and HT500 materials the PAG size is essentially the same.

The main microstructural difference among the three groups of specimens is the precipitate structure. Fig. 2 presents the results of SEM observations on carbon precipitate structure of the materials. In HT500 (Fig. 2(a) and (b)) the precipitates were mostly located inside the laths and the PAG boundaries were almost free of precipitates. With the tempering temperature increasing to 600 °C (HT600, Fig. 2(c) and (d)), dense and relatively small precipitates formed in the laths and also a lot of precipitates appeared at PAG and lath boundaries. With increasing tempering temperature to 760 °C (HT760, Fig. 2(e) and (f)), the coarsening of the precipitates occurred, while the density of precipitates inside the laths significantly decreased. More detailed analyses of the precipitate composition, structure, density and size distribution will be performed.

As reported in the literature [10], the hardness of ferritic/martensitic steels decreases with increasing tempering temperature. Fig. 3 shows the results of Vicker's micro-hardness (HV0.05) measurements. The trend agrees well with the published results (e.g. [10]), although the absolute values are slightly different, which should be due to the different compositions and heat treatments of the steels.

3.2. Tensile tests in Ar

In agreement with the micro-hardness results, the three groups of specimens demonstrated very different strengths. Fig. 4 presents the engineering stress–strain curves obtained at 300 °C in Ar. The HT600 and HT500 specimens have much higher strength than that of the HT760 specimen, as can also be seen in Fig. 5. All the curves exhibit ductile fracture behavior. It is interesting to note that the HT500 specimen showed not only very high strength but also a certain work hardening capability as the HT760 specimen, while the HT600 specimen indicated just the increase of strength and almost no work hardening capability. The higher strength of the HT500 and HT600 specimens can be attributed to the hardening effects of the carbon remained in solid solution and a high martensitic content. The little work hardening capacity of the HT600 specimens may be due to the dense and small precipitate structure, which may have a similar effect like defect-clusters or dislocation loops induced by irradiation.

The fracture morphology revealed that all the specimens tested in Ar exhibited a ductile fracture mode with fracture surfaces fully filled with dimples (Fig. 6(a), (c) and (e)).

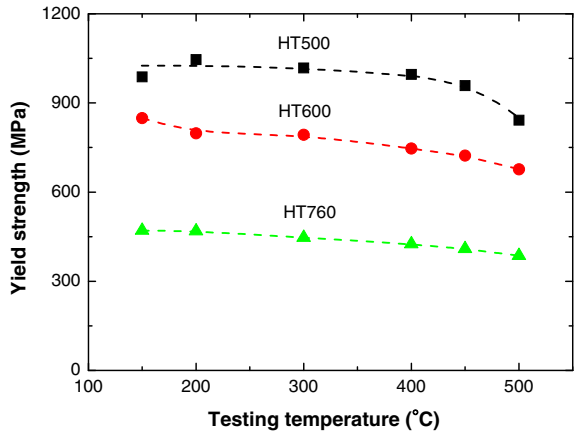

Fig. 5. Yield stress versus testing temperature for T91 tempered at different temperatures.

3.3. Tensile tests in LBE

Depending on testing temperature, the tensile properties of the HT500, HT600 and HT750 specimens exposed to LBE can be very different from that of the specimens tested in Ar.

Figs. 7–9 present the engineering stress–strain curves of these three groups of specimens tested in LBE at different temperatures. The results of the HT760 specimens (Fig. 7) indicate that the embrittlement phenomenon clearly appeared in a temperature range from 300 to 450 °C. The tensile curves of the specimens tested in this temperature range show fast failure of the specimens after necking started, which suggests that the LBE promoted the crack propagation. Although the total elongation was significantly reduced for these specimens, their yield and ultimate tensile strengths and uniform elongation were not affected.

The tensile test results of the HT600 samples are given in Fig. 8. One can see that the embrittlement is evident at temperatures between 150 and 400 °C. This temperature range is wider than that in HT760 case. Although the specimens did not break immediately after necking started, the fracture of these specimens took place at relatively low levels of deformation (elongation to fracture <8%).

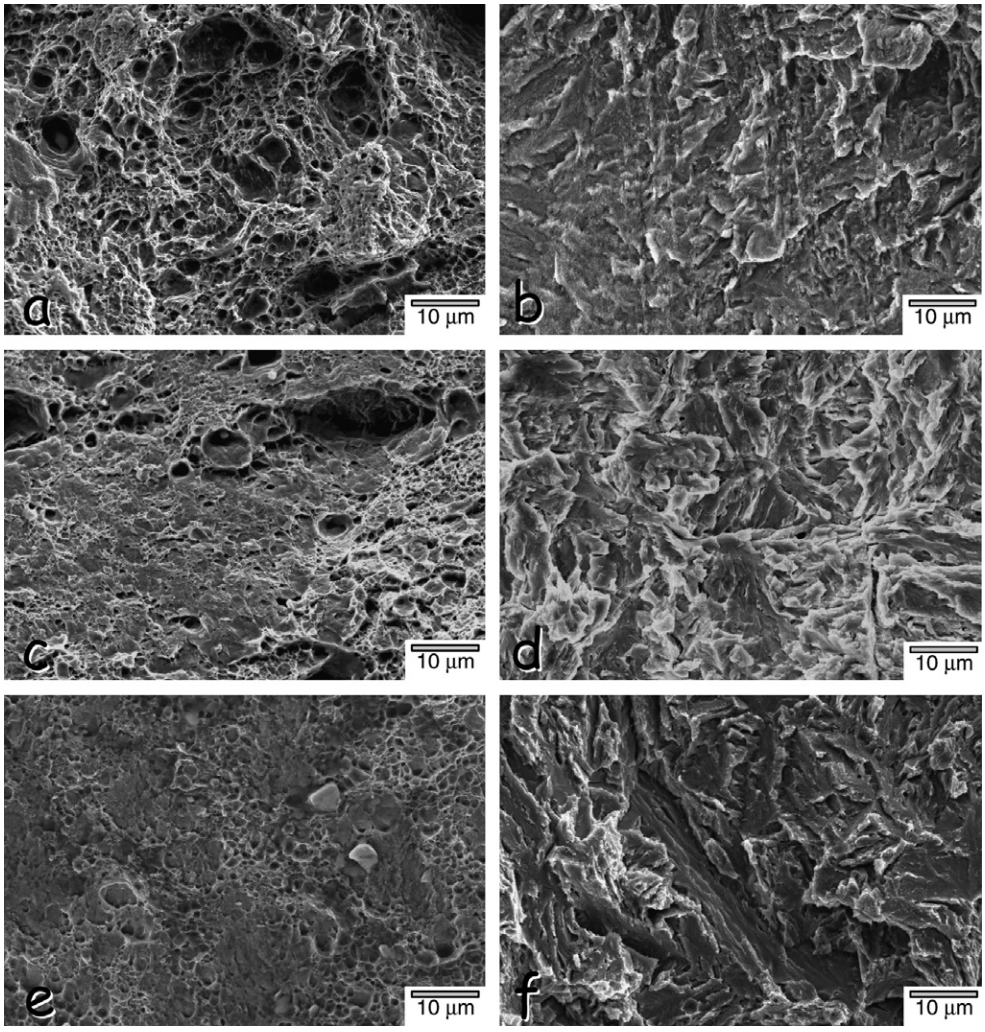

Fig. 6. SEM micrographs of the HT760, HT600 and HT500 specimens tested at 300 °C in Ar (graphs a, c, e, respectively) and in LBE (graphs b, d, f, respectively).

The tensile test results of the HT500 specimens (Fig. 9) reveal that the embrittlement started at 150 °C and continued up to450 °C and disappeared only at 500 °C. In this wide temperature range (150–450 °C), the specimens broke in a brittle manner before necking. Some specimens failed just after yielding.

These changes in tensile behaviors are also reflected by the features observed on the fracture surfaces of the specimens, which are also shown in Fig. 6 for a comparison with those of tests in Ar. The SEM micrographs presented in Fig. 6 for some specimens tested at 300 °C in both Ar and LBE demonstrate that the

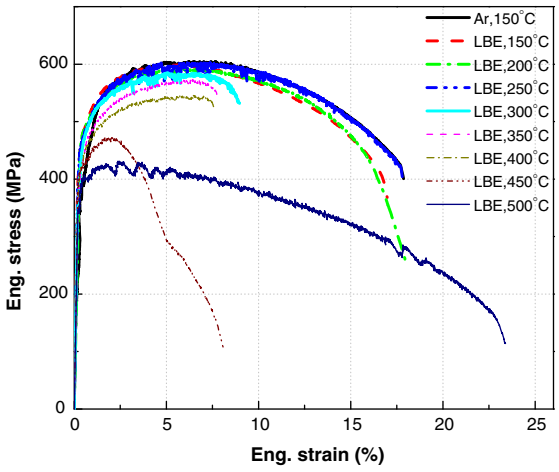

Fig. 7. Tensile stress–strain curves of the HT760 specimens tested in LBE and in Ar.

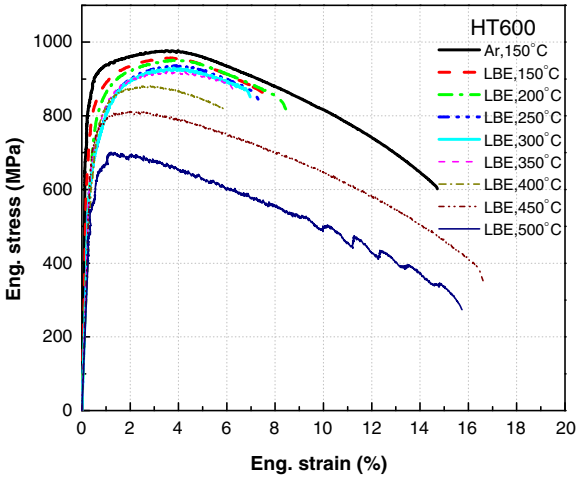

Fig. 8. Tensile stress–strain curves of the HT600 specimens tested in LBE and in Ar.

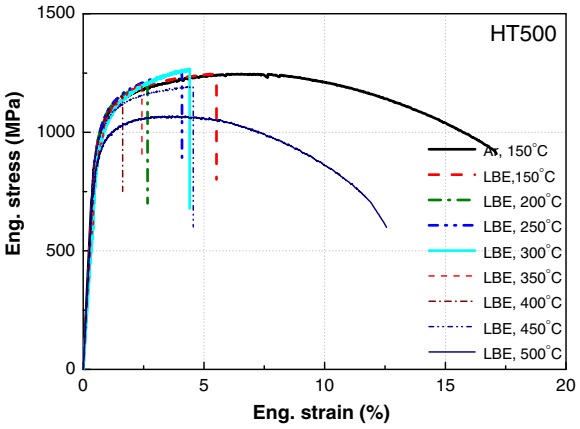

Fig. 9. Tensile stress–strain curves of the HT500 specimens tested in LBE and in Ar.

specimens tested in Ar broke in a typical ductile fracture mode, while the specimens tested in LBE ruptured in a brittle cleavage fracture mode.

4. Discussion

LME is normally a sort of temperature-dependent phenomena. A temperature range where LME appears is a so-called 'ductility-trough', which reflects the ductility degradation in the temperature range [1]. Fig. 10 summarizes the temperature dependences of the three groups of specimens tested in both Ar and LBE environments. One can see that the ductility-trough of the HT760 specimens is located between 300 and 450 °C. For the HT600 and HT500 specimens, the real onset of the ductility-trough is in fact not known, since no tests were performed at below 150 °C. From the trends of the HT600 and HT500 data, one can imagine that onset of the ductility-trough may be just above the melting point temperature of LBE (~125 °C). In the figure one can also see that the ductility-trough of the HT500 specimens is widest and deepest, while that of the HT760 specimens is narrowest and shallowest. This suggests that the width and depth of the ductility-trough increases with increasing strength of the specimens.

Although it is well known that hardened (e.g. by irradiation) FM steels are more brittle, the enhancing effect of high strength on LBE embrittlement is not yet understood. In the present work, it is believed that the fracture of the specimens resulted from the propagation of micro-cracks on the transverse surfaces, which were produced during EDM cutting [7]. All specimens tested in Ar environment ruptured in a ductile fracture mode. This indicates that the crack propagation in these specimens was through micro-void nucleation, growth and coalescence in front of crack tips, which resulted in transgranular fracture with dimples appearing on the fracture surfaces. The ductile fracture of these specimens means that the cleavage stress was not reached during all the tensile tests in Ar.

When the specimens were tested in an LBE environment, cleavage fracture appeared in the specimens tested in the ductility-trough temperature range. This indicates that the cleavage stress was reached or, more precisely, reduced in these specimens. The cleavage stress (σ_c) can be expressed with Cottrell's model as

$$\sigma_c = \left[\frac{4\mu\gamma_m}{\pi(1-\nu^2)}\right]^{1/2} d^{-1/2},$$

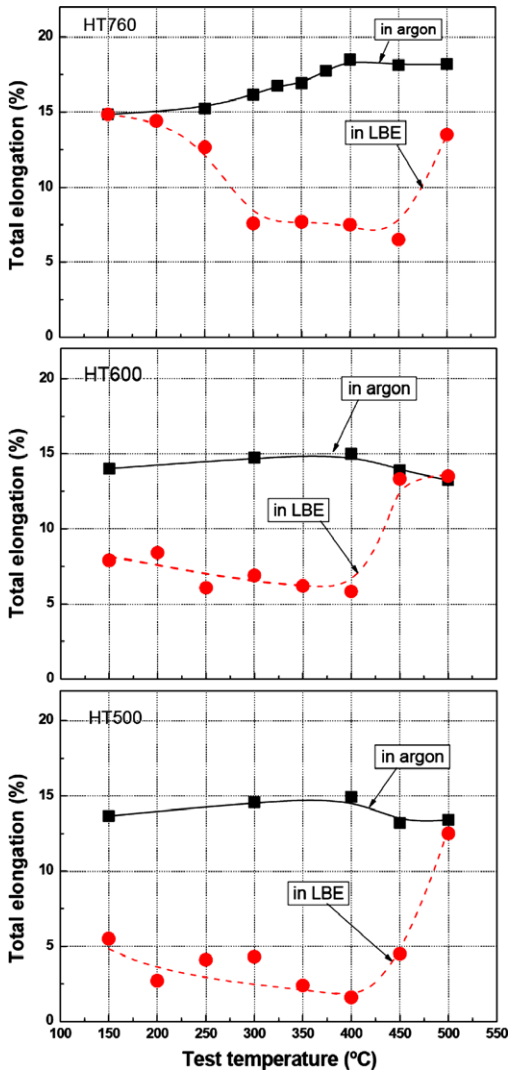

Fig. 10. Total elongation versus testing temperature for the HT760, HT600 and HT500 specimens tested in Ar and LBE.

where μ is the shear modulus, γ_m is the surface creation energy, ν is the Poisson ratio and d is the grain size. Except for the surface creation energy, all other parameters remained as the same during the tests in LBE and in Ar. Therefore, it can be concluded that the surface creation energy was reduced by LBE contacting. This agrees with a well accepted LME mechanism, the so-called 'weakening inter-atomic bond', namely the liquid metal atoms at a crack tip in steels would reduce the strength of the inter-atomic bonding and result in a decrease of the energy for creating new fracture surfaces.

Generally the stress concentration at a crack tip increases with increasing strength of the material. This means that the fracture stress level is relatively easy to be reached in the HT500 specimens and rather difficult to be reached in the HT760 specimens, and as a consequence the LBE embrittlement effect is more pronounced in the HT500 and HT600 specimens.

The detailed modeling work is ongoing and the results will be reported in the future.

5. Conclusion

In the present work, SSRT tests on T91 specimens in three tempering conditions (tempered at 500, 600 and 760 °C) were

conducted in Ar and in LBE at temperatures between 150 and 500 °C. The following conclusions are obtained.

(1) For the specimens in the normal tempering condition (tempered at 760 °C), the susceptibility to LBE embrittlement appeared in a temperature range of 300–450 °C.
(2) With increasing the strength of the steel by lowering the tempering temperature, specimens tempered at 600 and 500 °C demonstrated more pronounced embrittlement effects, reflected by wider and deeper ductility-troughs. This suggests that martensitic steels with higher strength are more susceptible to the LBE embrittlement.
(3) The LBE embrittlement effects can be attributed to the decrease of fracture stress resulted from the 'weakening interatomic bond' by LBE contacting at crack tips.

References

[1] B. Joseph, M. Picat, F. Barbier, Eur. Phys. J. – Appl. Phys. 5 (1999) 19.
[2] Y. Dai, in: Proceedings of the Sixth ESS General Meeting, vol. 3, Ancona, Italy, 20–23 September 1999.
[3] A. Legris, G. Nicaise, J. Vogt, J. Foct, D. Gorse, D. Vancon, Scr. Mater. 43 (2000) 997.
[4] C. Fazio, I. Ricapito, G. Scaddozzo, G. Benamati, J. Nucl. Mater. 318 (2003) 325.
[5] J.-B. Vogt, A. Verleene, I. Serre, A. Legris, J. Nucl. Mater. 335 (2004) 222.
[6] T. Auger, G. Lorang, S. Guérin, J.-L. Pastol, D. Gorse, J. Nucl. Mater. 335 (2004) 227.
[7] Y. Dai, B. Long, F. Groeschel, J. Nucl. Mater. 356 (2006) 222.
[8] Y. Dai, B. Long, X. Jia, H. Glasbrenner, K. Samec, F. Groeschel, J. Nucl. Mater. 356 (2006) 256.
[9] Y. Dai, J. Henry, T. Auger, J.-B. Vogt, A. Almazouzi, H. Glasbrenner, F. Groeschel, J. Nucl. Mater. 356 (2006) 308.
[10] R.L. Klueh, D.R. Harries, High-chromium Ferritic and Martensitic Steels for Nuclear Applications, ASTM, 2001 (Chapter 3).